CELL BIOLOGY

Locally translated mTOR controls axonal local translation in nerve injury

Marco Terenzio,[1] Sandip Koley,[1] Nitzan Samra,[1] Ida Rishal,[1] Qian Zhao,[2]* Pabitra K. Sahoo,[3] Anatoly Urisman,[2] Letizia Marvaldi,[1] Juan A. Oses-Prieto,[2] Craig Forester,[4] Cynthia Gomes,[3]† Ashley L. Kalinski,[3]‡ Agostina Di Pizio,[1] Ella Doron-Mandel,[1] Rotem Ben-Tov Perry,[1] Indrek Koppel,[1] Jeffery L. Twiss,[3,5] Alma L. Burlingame,[2] Mike Fainzilber[1]§

How is protein synthesis initiated locally in neurons? We found that mTOR (mechanistic target of rapamycin) was activated and then up-regulated in injured axons, owing to local translation of mTOR messenger RNA (mRNA). This mRNA was transported into axons by the cell size–regulating RNA-binding protein nucleolin. Furthermore, mTOR controlled local translation in injured axons. This included regulation of its own translation and that of retrograde injury signaling molecules such as importin β1 and STAT3 (signal transducer and activator of transcription 3). Deletion of the mTOR 3′ untranslated region (3′UTR) in mice reduced mTOR in axons and decreased local translation after nerve injury. Both pharmacological inhibition of mTOR in axons and deletion of the mTOR 3′UTR decreased proprioceptive neuronal survival after nerve injury. Thus, mRNA localization enables spatiotemporal control of mTOR pathways regulating local translation and long-range intracellular signaling.

Local translation enables spatiotemporal specificity in cell functions (*1*, *2*) such as the neuronal response to axon injury (*3*, *4*) or regrowth of injured axons (*5*, *6*). However, apart from a requirement for intra-axonal calcium (*7*), the mechanisms that regulate local protein synthesis in axons are largely unknown. mTOR, the mechanistic target of rapamycin, is a central regulator of translation (*8*), neuronal regeneration (*9*–*12*), and protein synthesis in neurons (*13*–*16*). We examined mTOR signaling in the sciatic nerve (SN) versus in dorsal root ganglia (DRG) after axonal injury and found differential phosphorylation of mTOR and associated signaling components (Fig. 1, A and B, and table S1). This suggested a specific role for mTOR in the early injury response in axons. We verified mTOR serine 2448 (S2448) phosphorylation (*17*) in axons by immunostaining, observing significant elevation within axons at 3 hours after injury, with a return to baseline at 12 hours (Fig. 1, C and D). We also observed that phosphorylation levels of EiF4b (S406), Akt (S473), S6 kinase (S6K; threonine 389), and ribosomal protein S6 (S240 and S244), all well-known effectors and regulators of mTOR signaling, increased rapidly after injury (Fig. 1E). Typically, Eif4b is activated in response to mTORC1, whereas Akt plays a role in both mTORC1 and mTORC2 signaling (*8*, *18*); hence, both mTOR complexes are activated locally by axonal injury.

We used the mTOR inhibitor torin-1 (fig. S1, A to C) to examine functions of local mTOR activation in nerve injury. Injection of torin-1 at the injury site before a conditioning SN lesion (*19*) reduced the subsequent lesion-induced axon outgrowth in culture (fig. S1, D and E). Neuron numbers recovered from torin-1–treated animals were also reduced (fig. S1F), so we examined the effects of torin-1 injection into the SN on proprioceptive neuron survival in DRG in vivo. Injecting torin-1 into the nerve concomitantly with injury reduced proprioceptive neuron numbers in the corresponding DRG (Fig. 1, F and G), supporting a role for axonal mTOR activation in neuronal injury response and survival. Examination of SN mTOR expression revealed unexpectedly low levels of mTOR protein in axons before injury. Axonal mTOR was markedly elevated in the vicinity of the lesion site up to 9 hours post-injury, which was followed by a decline back to baseline levels (Fig. 2A and fig. S2A). Up-regulation of mTOR in injured axons was further confirmed by immunoelectron microscopy on SN sections (fig. S2B).

The time frame of mTOR elevation in axons suggested that it might be synthesized locally. We examined this possibility by biotinylation of nascent synthesized proteins tagged with the puromycin derivative *O*-propargyl-puromycin (OPP) (*20*). We performed OPP incubation in rat nerve segments ex vivo, followed by axoplasm extraction (*21*), biotinylation, and precipitation with streptavidin (SA). Immunoblots of SA precipitates revealed robust de novo synthesis of mTOR, similar to that of importin β1, a well-established locally synthesized protein (*4*) (Fig. 2B). Immunostaining on mouse SN segments incubated ex vivo with the translation inhibitor cycloheximide indicated inhibition of axonal mTOR up-regulation (fig. S2, C and D), and fluorescent in situ hybridization (FISH) showed robust granular signals for mTOR mRNA in axons (fig. S2E). Direct visualization of de novo synthesized mTOR by puromycin labeling combined with a proximity ligation assay revealed robust signals for de novo synthesis of mTOR in sensory axons in culture (fig. S3, A to C). mTOR axonal up-regulation in nerve segments ex vivo and in culture was torin-1–sensitive (Fig. 2, C and D, and fig. S3, A to C), indicating that it is controlled by mTOR itself. Last, mTOR up-regulation after injury was mirrored by a decrease in axonal PTEN (fig. S3, D and E), a functional mTOR antagonist.

A complex comprising the RNA-binding protein (RBP) nucleolin and the kinesin motor Kif5A traffics importin β1 mRNA to axons (*22*). We tested for mTOR mRNA association with this complex by quantitative reverse transcription polymerase chain reaction (PCR) on immunoprecipitates of nucleolin or Kif5A from SN axoplasm. mTOR mRNA was robustly coprecipitated with both nucleolin and Kif5A (Fig. 2E and fig. S4, A and B). Furthermore, we observed significant colocalization of mTOR mRNA with nucleolin protein by combining FISH with immunostaining on sensory axons (Fig. 2, F and G). Last, restriction of nucleolin to neuronal somata by pretreatment of neuronal cultures with the DNA aptamer AS1411 (*22*) reduced mTOR mRNA in axons while increasing it in cell bodies (Fig. 2H and fig. S4, C and D), confirming that mTOR mRNA is transported to axons by the RBP nucleolin.

To assess the overall impact of mTOR on local translation in axons, we carried out puromycin labeling on SN segments preincubated with anisomycin, a general protein synthesis inhibitor, or with torin-1. We quantified puromycin incorporation into axonal proteins by immunostaining (Fig. 3, A and B) and capillary immunoelectrophoresis of axoplasm (Fig. 3, C and D). Torin-1 effectively inhibited axonal protein synthesis to a similar degree as anisomycin (Fig. 3, B and D). We then used OPP to characterize the ensemble of de novo synthesized proteins in axon injury by mass spectrometry (MS). SN segments were preincubated ex vivo with vehicle, anisomycin, or torin-1 and then pulsed with OPP before axoplasm extraction and biotinylation (fig. S5A). The efficiency of the reactions was assessed by immunoblotting with SA–horseradish peroxidase (HRP) (Fig. 3E). A cohort of ~550 proteins was identified after affinity purification and MS, of which 234 were affected equivalently by anisomycin or torin-1 pretreatments (Fig. 3F, fig. S5B, and table S2). Almost 80% of the torin-1–sensitive candidates were shared with the largest

[1]Department of Biomolecular Sciences, Weizmann Institute of Science, Rehovot 76100, Israel. [2]Department of Pharmaceutical Chemistry, University of California, San Francisco, CA 94158, USA. [3]Department of Biological Sciences, University of South Carolina, Columbia, SC 29208, USA. [4]Division of Pediatric Allergy, Immunology and Bone Marrow Transplantation, University of California, San Francisco, CA 94158, USA. [5]Department of Neurobiology and Anatomy, Drexel University College of Medicine, Philadelphia, PA 19129, USA.
*Present address: Department of Applied Biology and Chemical Technology, Hong Kong Polytechnic University, Hong Kong. †Present address: Department of Anatomical Sciences and Neurobiology, University of Louisville, KY 40202, USA. ‡Present address: Department of Cell and Developmental Biology, University of Michigan Medical School, 109 Zina Pitcher Place, Ann Arbor, MI 48188, USA.
§Corresponding author. Email: mike.fainzilber@weizmann.ac.il

known translatome data set of mTOR-regulated survival-promoting mRNAs (*23*, *24*) (fig. S5C). The mTOR-dependent axonally synthesized proteins included many known axonal injury response proteins (*25*) (table S2), leading us to test the effect of torin-1 on injury-induced axonal up-regulation of STAT3 (signal transducer and activator of transcription 3; Fig. 3, G and H), importin β1 (fig. S5, D and E), and vimentin (fig. S5, F and G). Locally translated STAT3 is phosphorylated in sensory axons as a retrograde survival signal (*26*), so we also tested the effect of torin-1 on phospho-STAT3 (Fig. 3, G and H). Torin-1 effectively inhibited the localized axonal elevation of all the tested injury-signaling proteins, indicating that local translation for retrograde injury signaling is controlled by mTOR in sensory axons.

The findings above suggest that axonal localization of mTOR mRNA enables subcellular regulation of axonal protein synthesis. Localization motifs are often located in the 3′ untranslated regions (3′UTRs) of axonal mRNAs (*27*), and axonal localization was previously reported for the mTOR 3′UTR (*15*). We sequenced 3′RACE (rapid amplification of cDNA ends) PCR products and identified a single major mTOR 3′UTR sequence, as expected from genome annotation. The mTOR 3′UTR effectively localized green fluorescent protein mRNA to axons in transfected neurons (fig. S6, A and B). We then removed most of the 3′UTR sequence from the mTOR locus by using CRISPR-Cas9 gene editing (fig. S6C and table S3), without affecting the open reading frame or other elements of the gene. We verified that the segment targeted for deletion had axon-localizing capacity (mTOR 3′UTR 54 to 789), whereas segments predicted to be retained in the mutant mouse lacked axon-localizing capacity (mTOR 3′UTR 1 to 69 and 774 to 825; fig. S6, A and B). mTOR 3′UTR–null mice were viable, and 3′RACE analyses of homozygous null DRG neurons confirmed the deletion (fig. S6D).

FISH analyses of SN sections revealed a significant reduction in axonal mTOR mRNA levels in vivo in the SN of mTOR 3′UTR–null mice (Fig. 4, A and B, and fig. S6E), with no significant changes in stability or half-life of mTOR mRNA or protein (fig. S7). Ex vivo incubation of mTOR 3′UTR–null SN segments showed a large reduction in injury-induced mTOR protein up-regulation compared with the wild type (Fig. 4, C and D). Cultures of 3′UTR-null neurons revealed little or no change in mTOR protein levels in the soma, whereas mTOR protein levels in the growth cones and axon tips were significantly reduced (fig. S8, A and B). These subcellular effects on mTOR protein up-regulation were mirrored in mTOR downstream signaling, with no change in phospho-S6 levels in the somata of 3′UTR-null neurons, in contrast to a marked deficit in phospho-S6 up-regulation in injured axons from the mutant mice (fig. S8, C and D).

We then examined effects of the mTOR 3′UTR deletion on axonal protein synthesis and on the mTOR-dependent injury response in lesioned DRG neurons. Puromycinylation experiments in

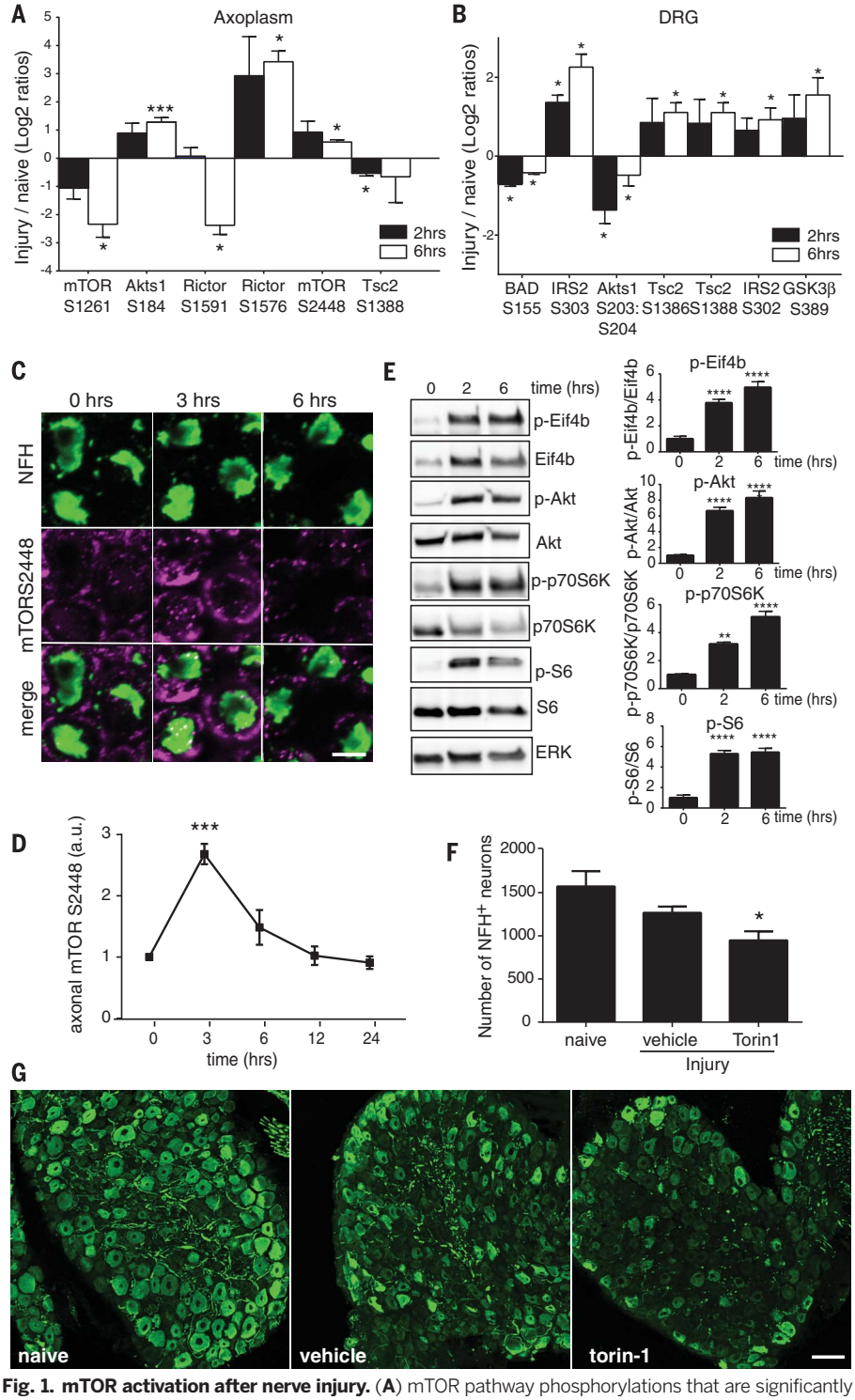

Fig. 1. mTOR activation after nerve injury. (**A**) mTOR pathway phosphorylations that are significantly regulated by SN injury ($n = 3$; means ± SEM; $^*P < 0.05$, $^{***}P < 0.001$; t test). (**B**) As in (A), for L4/L5 DRG ($n = 3$; means ± SEM; $^*P < 0.05$; t test). (**C**) SN sections stained for the axonal marker NFH (green) and mTOR S2448 (magenta), naive versus 3 and 6 hours after injury. Scale bar, 5 μm. (**D**) Axonal mTOR S2448 over time after injury, normalized to naive conditions [$n = 3$; means ± SEM; $^{***}P < 0.001$; one-way analysis of variance (ANOVA) with Bonferroni's post-test]. a.u., arbitrary units. (**E**) Immunoblots of phospho-EIF4b, -Akt, -S6K, and -S6 and the corresponding total proteins in SN axoplasm over time after injury. Quantifications are shown on the right ($n = 4$; means ± SEM; $^{**}P < 0.01$, $^{****}P < 0.0001$; one-way ANOVA with Bonferroni's post-test). (**F** and **G**) SNs were injected with vehicle or torin-1 before injury, and L4 DRG were harvested 7 days later, serially sectioned at 20-μm intervals, and stained for NFH (green) to allow counting of proprioceptive neurons. Quantifications of NFH-positive neuron numbers per DRG are shown in (F) ($n = 7$; means ± SEM; $^*P < 0.05$; t test); representative images are in (G) (scale bar, 50 μm).

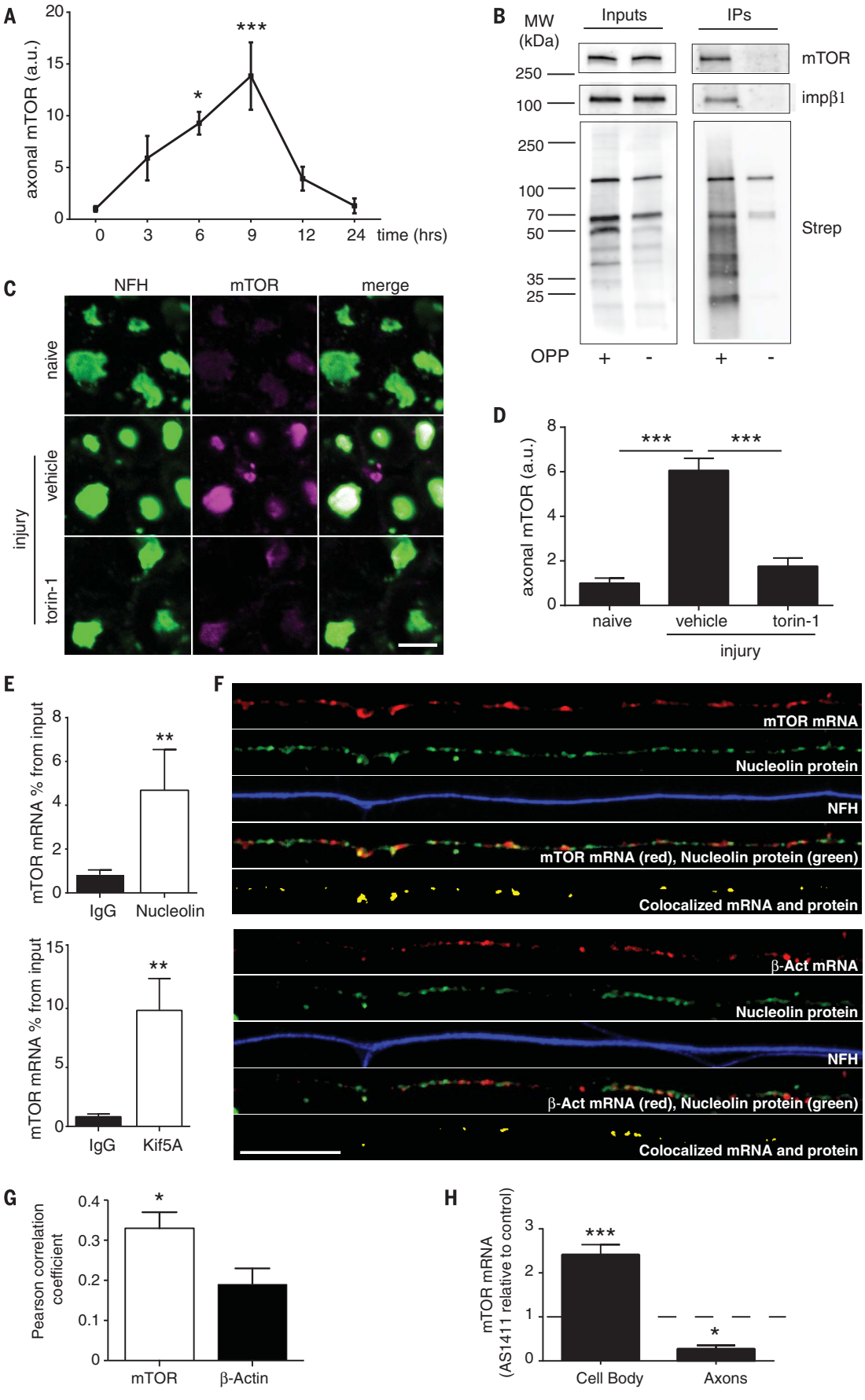

Fig. 2. mTOR is locally translated after SN injury. (**A**) mTOR regulation over time after injury at the SN lesion site ($n = 5$; means ± SEM; $^*P < 0.05$, $^{***}P < 0.001$; one-way ANOVA with Bonferroni's post-test). (**B**) Immunoblots reveal newly synthesized mTOR and importin β1 (Impβ1) from OPP-treated rat SNs, confirming their local translation after injury. IPs, immunoprecipitates; Strep, streptavidin. (**C**) Torin-1 (4 μM) effects on mTOR up-regulation in sections from SN 4 hours ex vivo, stained for NFH (green) and mTOR (magenta). Scale bar, 5 μm. (**D**) Quantification of axonal mTOR from (C) ($n = 6$; means ± SEM; $^{***}P < 0.001$; one-way ANOVA with Bonferroni's post-test). (**E**) Quantification of mTOR transcript levels after pulldown for Kif5A or nucleolin in axoplasm (percent from input; $n = 6$; means ± SEM; $^{**}P < 0.01$; ratio paired t test). IgG, immunoglobulin G. (**F**) Representative epifluorescent images for colocalization of endogenous mTOR or β-actin transcripts, visualized by in situ hybridization (red), and nucleolin protein, visualized by immunostaining (green). Axons were visualized by neurofilament immunostaining (blue). Scale bar, 10 μm. (**G**) Pearson's correlation coefficient for mTOR mRNA colocalization with nucleolin (0.33 ± 0.04; $n = 24$) differs significantly from that for β-actin mRNA colocalization with nucleolin (0.19 ± 0.04; $n = 20$). $^*P < 0.05$; t test. (**H**) Quantification of relative mTOR transcript levels in cell bodies and axons of neurons treated with AS1411 versus control aptamer, plotted as the fold change over control aptamer. 18S RNA served as an internal control ($n = 3$; means ± SEM; $^*P < 0.05$, $^{***}P < 0.001$; unpaired two-sample t test).

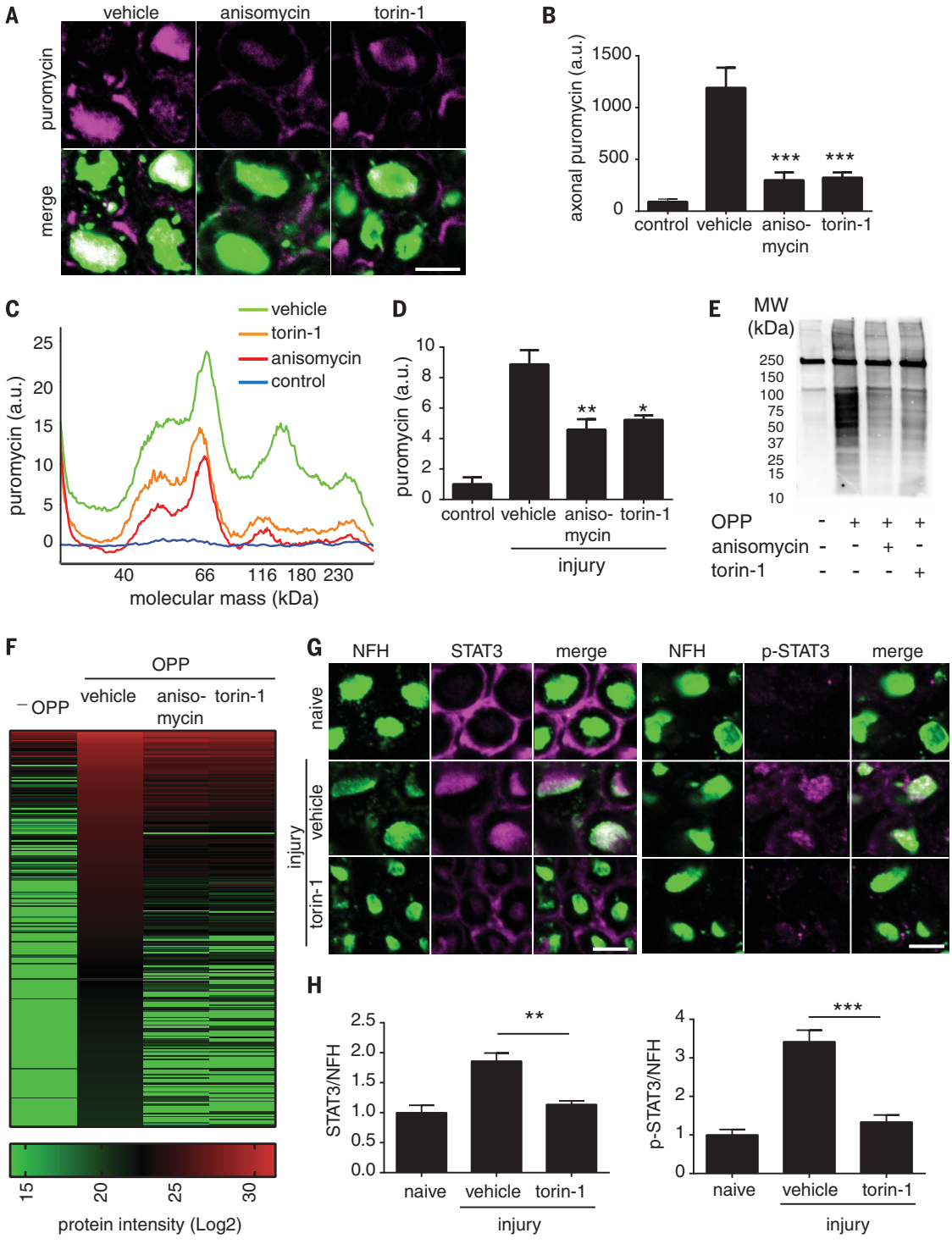

Fig. 3. mTOR regulates axonal local translation after SN injury. (**A**) SN segments 2 hours ex vivo with anisomycin (200 μg/ml), torin-1 (4 μM), or vehicle, followed by 1 hour with puromycin (100 μg/ml), sectioned and stained for NFH (green) and puromycin (magenta). Scale bar, 5 μm. (**B**) Quantification of axonal puromycin in the experiment described in (A) (n = 5; means ± SEM; ***P < 0.001; one-way ANOVA with Bonferroni's post-test). (**C**) Representative runs of puromycinylated proteins in SN axoplasm from the experiment described in (A), analyzed by capillary immunoelectrophoresis. (**D**) Quantification of (C) (n = 4; means ± SEM; *P < 0.05, **P < 0.01; ANOVA with Bonferroni's post-test). (**E**) SA-HRP immunoblots of OPP-biotin–labeled axoplasm samples before MS. (**F**) Heat map of OPP-biotin–labeled protein candidates identified by MS. (**G**) SN segments 4 hours ex vivo with torin-1 (4 μM) or vehicle (dimethyl sulfoxide), sectioned and stained for NFH (green) and STAT3 or phospho-STAT3 (both magenta). Scale bars, 5 μm. (**H**) Quantification of axonal STAT3 and phospho-STAT3 for the experiment described in (G) (n = 4; means ± SEM; **P < 0.01, ***P < 0.001; one-way ANOVA with Bonferroni's post-test).

SN segments ex vivo showed a clear reduction in puromycin incorporation in mTOR 3′UTR–null axons (Fig. 4, E and F, and fig. S9, A to D). SN injury in mutant mice led to reductions in L4 DRG proprioceptive neuron numbers 7 days later, to a similar degree as we previously observed for torin-1 injection concomitant with injury (Fig. 4I and fig. S9E). We tested whether the observed effects were indeed due to the loss of mTOR up-regulation in injured axons by injecting recombinant mTOR protein into the nerve concomitantly with injury. Exogenously supplied mTOR protein restored both local axonal translation (Fig. 4, G and H) and neuronal survival (Fig. 4I and fig. S9E) in the mutant mice. Thus, removal of the mTOR 3′UTR reduces axonal localization of mTOR mRNA and attenuates local elevation of mTOR protein in injured axons. Subcellular reduction in axonal mTOR affects overall local protein synthesis in injured axons and reduces the survival of lesioned neurons.

Maintenance of a latent and silent axonal pool of mTOR in mRNA form enables rapid and local up-regulation of protein synthesis upon need. The linkage of mTOR mRNA transport to nucleolin likely explains nucleolin regulation of subcellular protein synthesis in cell size regulation (*22*). Regulation of mTOR pathways through mRNA localization may have impacts on many aspects of

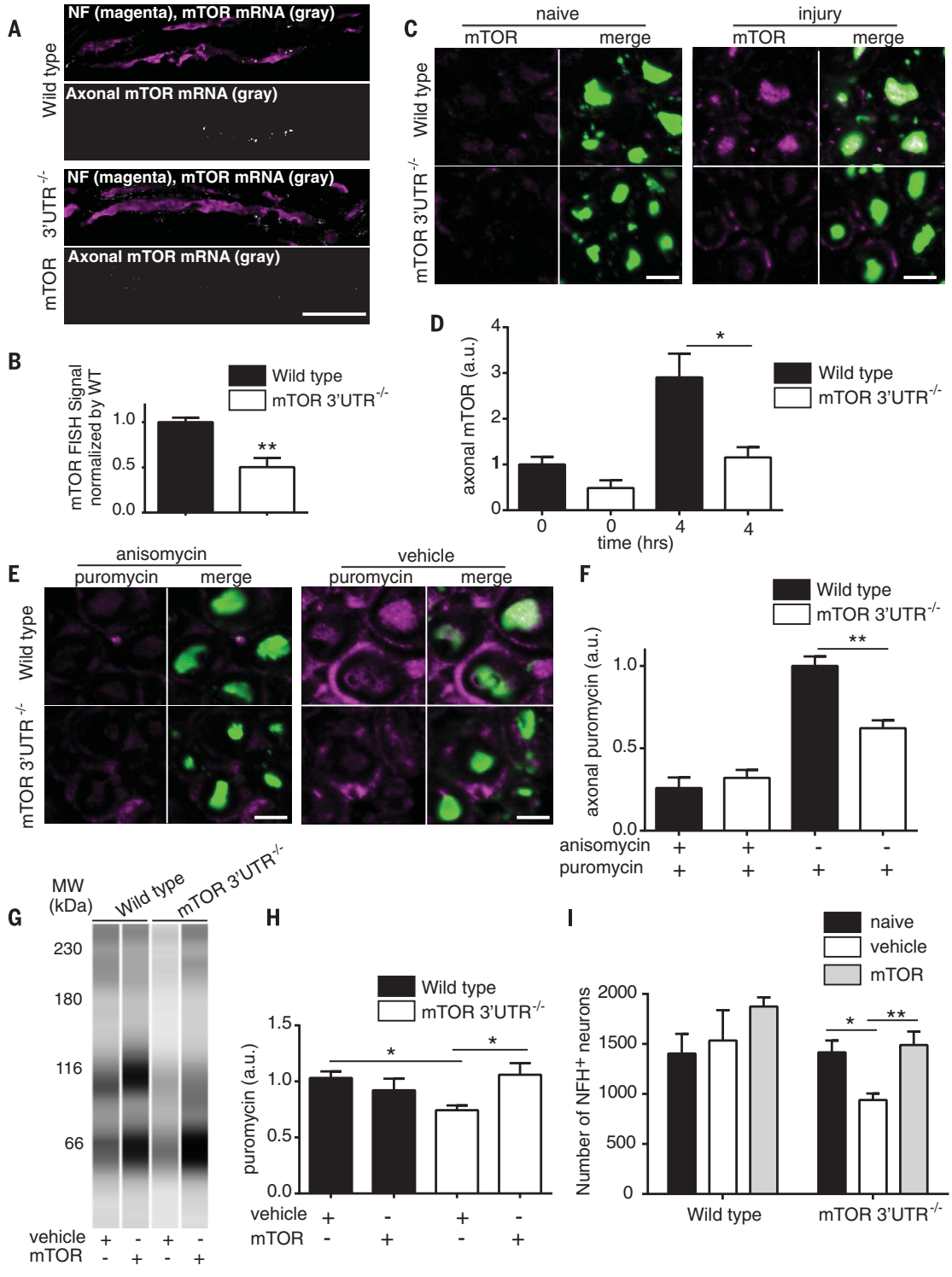

Fig. 4. Effects of mTOR 3′UTR deletion. (**A**) Representative, exposure-matched confocal images of FISH (Stellaris) for mTOR mRNA and neurofilament (NF) immunostaining from SN sections of wild-type and mTOR 3′UTR$^{-/-}$ mice. Upper panels show single optical planes for merged NFH and mTOR channels. Lower panels show single optical planes of mTOR mRNA pixels that overlap with NFH and were projected to a separate channel as "axon only" mTOR signals. Scale bar, 10 μm. (**B**) Quantification of (A) reveals a ~50% reduction in axonal mTOR in the 3′UTR$^{-/-}$ mice (n = 4; means ± SEM; $^{**}P < 0.01$; unpaired t test). WT, wild type. (**C**) SN segments from the indicated genotypes 4 hours ex vivo, sectioned and stained for NFH (green) and mTOR (magenta). Scale bars, 5 μm. (**D**) Quantification of (C) (n = 3; means ± SEM; $^{*}P < 0.05$; one-way ANOVA with Bonferroni's post-test). (**E**) SN segments from the indicated genotypes 2 hours ex vivo with anisomycin (200 μg/ml) or vehicle, followed by 1 hour with puromycin (100 μg/ml), then sectioned and stained as indicated. Scale bars, 5 μm. (**F**) Quantification of (E) (n = 3; means ± SEM; $^{**}P < 0.01$; one-way ANOVA with Bonferroni's post-test). (**G**) SN segments from wild-type and mTOR 3′UTR$^{-/-}$ mice not injected, injected with vehicle, or injected with 350 ng of mTOR protein were incubated in DMEM 2 hours ex vivo, followed by 1 hour of puromycin (100 μg/ml) treatment. A representative pseudoblot of puromycinylated proteins in SN axoplasm analyzed by capillary immunoelectrophoresis is shown. (**H**) Quantification of (G) (n = 4; means ± SEM; $^{*}P < 0.05$; one-way ANOVA with Bonferroni's post-test). (**I**) SNs from wild-type and mTOR 3′UTR$^{-/-}$ mice were injected with either vehicle or 350 ng of mTOR protein concomitantly with crush injury. L4 DRGs connected to the injured SN were harvested 7 days after injury, serially sectioned at 20-μm intervals, and stained for the proprioceptive marker NFH. Naive L4 DRG were also processed as a reference. Shown are the number of NFH-positive neurons per DRG (n = 4; means ± SEM; $^{*}P < 0.05$, $^{**}P < 0.01$; one-way ANOVA with Tukey's post-test).

neuronal physiology apart from injury, because localized changes in mTOR activity affect diverse processes, including viral latency (*28*), autophagy (*29*), and synaptic plasticity (*30*). Intracellular localization of mTOR at the protein level is well established in non-neuronal cells (*31*–*33*). mTOR localization at the RNA level provides an additional mode of spatiotemporal regulation of its pathways, with potentially broad physiological implications.

REFERENCES AND NOTES

1. V. Rangaraju, S. tom Dieck, E. M. Schuman, *EMBO Rep.* **18**, 693–711 (2017).
2. M. Terenzio, G. Schiavo, M. Fainzilber, *Neuron* **96**, 667–679 (2017).
3. S. Hanz *et al.*, *Neuron* **40**, 1095–1104 (2003).
4. R. B.-T. Perry *et al.*, *Neuron* **75**, 294–305 (2012).

5. J. Q. Zheng *et al*., *J. Neurosci.* **21**, 9291–9303 (2001).
6. C. J. Donnelly *et al*., *EMBO J.* **30**, 4665–4677 (2011).
7. D. Yudin *et al*., *Neuron* **59**, 241–252 (2008).
8. B. D. Fonseca *et al*., *Semin. Cell Dev. Biol.* **36**, 102–112 (2014).
9. K. K. Park *et al*., *Science* **322**, 963–966 (2008).
10. N. Abe, S. H. Borson, M. J. Gambello, F. Wang, V. Cavalli, *J. Biol. Chem.* **285**, 28034–28043 (2010).
11. X. Duan *et al*., *Neuron* **85**, 1244–1256 (2015).
12. W. Chen *et al*., *eNeuro* **3**, ENEURO.0358-16.2016 (2016).
13. K. F. Raab-Graham, P. C. Haddick, Y. N. Jan, L. Y. Jan, *Science* **314**, 144–148 (2006).
14. N. M. Sosanya *et al*., *J. Cell Biol.* **202**, 53–69 (2013).
15. M. J. Kye *et al*., *Hum. Mol. Genet.* **23**, 6318–6331 (2014).
16. N. G. Gracias, N. J. Shirkey-Son, U. Hengst, *Nat. Commun.* **5**, 3506 (2014).
17. O. Meyuhas, *Int. Rev. Cell Mol. Biol.* **320**, 41–73 (2015).
18. R. A. Saxton, D. M. Sabatini, *Cell* **168**, 960–976 (2017).
19. D. S. Smith, J. H. Skene, *J. Neurosci.* **17**, 646–658 (1997).
20. C. M. Forester *et al*., *Proc. Natl. Acad. Sci. U.S.A.* **115**, 2353–2358 (2018).
21. I. Rishal *et al*., *Dev. Neurobiol.* **70**, 126–133 (2010).
22. R. B. Perry *et al*., *Cell Rep.* **16**, 1664–1676 (2016).
23. V. Gandin *et al*., *Genome Res.* **26**, 636–648 (2016).
24. O. Meyuhas, T. Kahan, *Biochim. Biophys. Acta* **1849**, 801–811 (2015).
25. I. Rishal, M. Fainzilber, *Nat. Rev. Neurosci.* **15**, 32–42 (2014).
26. K. Ben-Yaakov *et al*., *EMBO J.* **31**, 1350–1363 (2012).
27. C. Andreassi, A. Riccio, *Trends Cell Biol.* **19**, 465–474 (2009).
28. M. Kobayashi, A. C. Wilson, M. V. Chao, I. Mohr, *Genes Dev.* **26**, 1527–1532 (2012).
29. D. Ebrahimi-Fakhari *et al*., *Cell Rep.* **17**, 1053–1070 (2016).
30. T. J. Younts *et al*., *Neuron* **92**, 479–492 (2016).
31. C. Betz, M. N. Hall, *J. Cell Biol.* **203**, 563–574 (2013).
32. Y. Sancak *et al*., *Cell* **141**, 290–303 (2010).
33. M. Ebner, B. Sinkovics, M. Szczygieł, D. W. Ribeiro, I. Yudushkin, *J. Cell Biol.* **216**, 343–353 (2017).

ACKNOWLEDGMENTS

We thank D. Gordon, N. Korem, A. Lin, N. Okladnikov, and E. Kanevskaya for excellent assistance; V. Kiss and V. Shinder for professional microscopy support; S. Ben-Dor for help with guide RNA design; R. Haffner-Krausz for mouse genome editing; and R. Rotkopf for statistical consultations. **Funding:** This work was supported by funding from the European Research Council (Neurogrowth, to M.F.), the Dr. Miriam and Sheldon G. Adelson Medical Research Foundation (to M.F., J.L.T., and A.L.B.), the Minerva Foundation (to M.F.), the Israel Science Foundation (1284/13 to M.F.), the Department of Defense Congressionally Mandated Research Program (W81XWH-2013-1-308 OR120042 to J.L.T. and M.F.), the National Institutes of Health (R01-NS041596 to J.L.T. and GM103481 to A.L.B.), and the Company of Biologists (*Journal of Cell Science* travel grants to I.K. and N.S.). M.T. was supported by a Koshland senior postdoctoral fellowship. M.F. is the incumbent of the Chaya Professorial Chair in Molecular Neuroscience at the Weizmann Institute of Science. J.L.T. is the incumbent of the SmartState Chair in Childhood Neurotherapeutics at the University of South Carolina. **Author contributions:** M.F. and M.T. designed the study. M.T., S.K., N.S., I.R., Q.Z., P.K.S., A.U., L.M., J.A.O.-P., C.G., A.L.K., A.D.P., R.B.-T.P., E.D.-M., and I.K. performed experiments and data analyses. Q.Z., C.F., A.U., and J.A.O.-P. carried out MS analyses. P.K.S., C.G., and A.L.K. conducted FISH analyses. I.R. performed electron microscopy. M.F., J.L.T., and A.L.B. supervised research. M.F. and M.T. wrote the initial manuscript draft. All authors revised the manuscript and approved the final version. **Competing interests:** None declared. **Data and materials availability:** All data needed to evaluate the conclusions of the paper are present in the paper and/or the supplementary materials.

SUPPLEMENTARY MATERIALS

www.sciencemag.org/content/359/6382/1416/suppl/DC1
Materials and Methods
Figs. S1 to S9
Tables S1 to S3
References (*34*–*51*)

5 March 2017; resubmitted 13 December 2017
Accepted 30 January 2018
10.1126/science.aan1053

Locally translated mTOR controls axonal local translation in nerve injury

Marco Terenzio, Sandip Koley, Nitzan Samra, Ida Rishal, Qian Zhao, Pabitra K. Sahoo, Anatoly Urisman, Letizia Marvaldi, Juan A. Oses-Prieto, Craig Forester, Cynthia Gomes, Ashley L. Kalinski, Agostina Di Pizio, Ella Doron-Mandel, Rotem Ben-Tov Perry, Indrek Koppel, Jeffery L. Twiss, Alma L. Burlingame and Mike Fainzilber

Science **359** (6382), 1416-1421.
DOI: 10.1126/science.aan1053

Local control of localized protein synthesis

Localized protein synthesis provides spatiotemporal precision for injury responses and growth decisions at remote positions in nerve axons. Terenzio *et al.* show that this process is controlled by local translation of preexisting axonal mRNA encoding the master regulator mTOR (see the Perspective by Riccio). mTOR controls both its own synthesis and that of most newly synthesized proteins at axonal injury sites, thereby determining the subsequent survival and growth of the injured neuron.

Science, this issue p. 1416; see also p. 1331

Science (print ISSN 0036-8075; online ISSN 1095-9203) is published by the American Association for the Advancement of Science, 1200 New York Avenue NW, Washington, DC 20005.